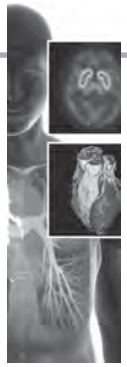

Correlation between diffusion tensor imaging and histological brain injury in ventilated preterm lambs

Objective: Inflammation and mechanical ventilation contribute additively to white matter injury in the preterm infant. We examined whether *in vivo* diffusion tensor imaging (DTI) indices correlate with immunohistochemical analyses of brain inflammation and injury caused by injurious ventilation at birth, in the presence or absence of intrauterine inflammation.

Methods: Twin-bearing ewes received an ultrasound guided injection of lipopolysaccharide (LPS; n=11) or saline (n=12) 7 days prior to delivery at ~125 days gestation. Immediately after delivery, lambs received either an injurious (LPS+INJ; n=5 and INJ; n=6) or protective (LPS+PROT; n=6 and PROT; n=5) ventilation strategy for 90 min, after which DTI was assessed. Following imaging, neuronal density (NeuN antibody) in the thalamus (Th) and myelin density (myelin basic protein, MBP) in the internal capsule (IC) and periventricular white matter (PVWM) were assessed.

Results: LPS exposure significantly increased axial diffusivity (P=0.01) and decreased myelin density in the IC (P=0.02) compared to saline groups. Moreover, there was a strong inverse correlation between fractional anisotropy values and myelin density in PVWM (P=0.01), and a trend in the IC (P=0.07) in all lambs. Injurious ventilation tended to reduce radial and mean diffusivity in the Th (P=0.07 and P=0.08).

Conclusion: DTI was able to detect microstructural changes associated with a reduction in myelination due to inflammation in the short term. However, DTI indices were not sensitive enough to consistently detect the microstructural changes induced by injurious ventilation immediately after birth.

KEYWORDS: brain injury ▪ MRI ▪ neonate ▪ neuroimaging ▪ preterm ▪ ventilation

Introduction

Many preterm neonates require mechanical ventilation immediately after birth to facilitate lung aeration and gas exchange, and to trigger the cardiovascular transition [1]. Despite the necessity of resuscitation, the initiation of mechanical ventilation can cause brain injury in preterm neonates, particularly if delivered with injurious high tidal volumes [2,3]. Intrauterine inflammation (chorioamnionitis) is an antecedent of preterm birth and is present in up to two-thirds of extremely preterm infants [4]. Chorioamnionitis increases white matter injury and confers a four-fold increased risk of cerebral palsy [5,6]. Given the frequency of chorioamnionitis and the high requirement for mechanical ventilation, a large proportion of preterm infants are exposed to both intrauterine inflammation and mechanical ventilation. Preclinical studies have revealed that this combination of risk factors exacerbates brain inflammation and the resultant injury, which can be detected histologically within the first hours after birth [7,8].

There is a critical need for non-invasive early detection of brain injury in preterm infants, which may be provided by advanced magnetic resonance imaging (MRI). We have previously shown that diffusion tensor imaging (DTI) is able to detect early brain injury using a region of interest (ROI) analysis [9]. Furthermore, our DTI colour map threshold approach detected subtle brain injuries caused by mechanical ventilation following ongoing intrauterine inflammation induced by subacute (7 days) exposure to intra-amniotic (IA) lipopolysaccharide (LPS) [10]. In the current study, we examined whether *in vivo* MRI indices correlate with immunohistochemical analyses of brain inflammation and injury following high tidal volume (V_T) injurious ventilation in the presence or absence of intrauterine inflammation. We hypothesised that alteration in fractional anisotropy and diffusivity correlate with histopathological observations of white matter injury caused by injurious mechanical ventilation at the time of preterm delivery. We also hypothesised that these indices of brain injury are exacerbated in preterm lambs exposed to intrauterine inflammation.

Dhafer M Alahmari[1,2], Samantha K Barton[3], Robert Galinsky[3], Ilias Nitsos[3], Anzari Atik[3], Michael Farrell[1,2], James Todd Pearson[2,4,5*#] & Graeme R Polglase[3,4#]

[1]Department of Medical Imaging and Radiation Sciences, Monash Biomedicine Discovery Institute, Monash University, Australia

[2]Monash Biomedical Imaging, Monash University, Australia

[3]Department of Obstetrics and Gynaecology, The Ritchie Centre, Hudson Institute of Medical Research, Monash University, Clayton, VIC, Australia

[4]Department of Physiology, Monash University, Clayton, VIC, Australia

[5]Department of Cardiac Physiology, National Cerebral and Cardiovascular Center, Suita, Osaka, Japan

[#]Authors contributed equally

**Author for correspondence:*

jpearson@ncvc.go.jp

Methods

■ Ethics statement

The experimental protocol was approved by Monash Medical Centre animal ethics committee (MMCA) at Monash University, and conducted in accordance with guidelines established by the National Health and Medical Research Council of Australia.

■ LPS treatment of the fetus, preterm delivery and stabilisation

The instrumentation and delivery of preterm lambs have been described in detail previously [3,7,10]. Briefly, one amniotic sac in twin-bearing ewes received an ultrasound guided injection of LPS (n=11) and the other saline (n=12) at 118 ± 2 days gestational age. Seven days later, at 125 ± 2 days gestational age, ewes were anaesthetised (isoflurane 1.5-3.0% in 100% O_2, Bomac Animal Health, NSW, Australia) and lambs delivered. Lambs exposed to LPS were identified by thickened fetal membranes and the presence of funisitis. Lambs were then delivered, dried, weighed and placed under a radiant heater, and ventilated as detailed below. Polyvinyl catheters (ID 0.86 mm, OD 1.52 mm, Dural Plastics, Australia) were placed in an umbilical artery and vein to monitor mean arterial pressure and to maintain anaesthesia, respectively. Spontaneous breathing was minimised by sedation of the lambs (Alfaxane i.v. 5-15 mg/kg/h; Jurox, East Tamaki, Auckland, New Zealand) during the experiment. Core body temperature was monitored via a rectal thermometer and temperature was regulated to 38-39°C; normal body temperature of lambs. Ewes were humanly killed (sodium pentobarbitone: 100 mg/kg i.v.) after caesarean section.

■ Resuscitation strategy

We utilised two ventilation strategies, as recently described by us [9,10]. Lambs in the injurious groups (LPS+INJ; n=5 and INJ; n=6) received 15 min of high V_T ventilation targeting 12-15 mL/kg with a maximum peak inflation pressure (PIP) set at 50 cm H_2O using a neonatal positive pressure ventilator (Babylog 8000+, Dräger, Lübeck, Germany). For the remaining 75 min, INJ lambs were ventilated using volume guaranteed ventilation set at 7 mL/kg. Lambs receiving the protective strategy (LPS+PROT; n=6 and PROT; n=5) received prophylactic surfactant (100 mg/kg, Curosurf®, Chiesi Pharma, Italy) followed by a 30 seconds sustained inflation (Neopuff, Fisher & Paykel Healthcare, Auckland, New Zealand) at PIP 35 cm H_2O. About 1 h after delivery, lambs were transferred onto a MR compatible ventilator (Pneupac, Smiths Medical, UK) and moved to the MR scanner.

Magnetic Resonance Imaging Protocol

We utilised MRI acquisition protocols as published previously by us [9,10]. Imaging studies were performed at Monash Biomedical Imaging, Monash University (Clayton, Australia). Imaging was performed using a 3T MR scanner (Siemens Skyra, Erlangen, Germany), with a 15-channel radio frequency (RF) coil for both RF transmission and reception. The MRI technologist and supporting team were blinded to group treatment for each lamb during MRI examination. Lambs were scanned in a supine position and heart rate, SpO_2 and blood gas parameters monitored regularly to maintain lamb well-being.

After conventional structural (T_1,T_2) and susceptibility weighted imaging (SWI), DTI data were acquired using a spin-echo echo planar imaging (EPI) sequence. Depending on the size of the brain ~50 contiguous 1.2 mm axial slices were obtained covering the brain. The brains from lambs in all groups were imaged using 30 directions with a b value of 1,000 s/mm^2 (TR=11,400 ms, TE=99 ms). The data matrix was 128*128, collected from a FOV of 154 mm*154 mm, giving a voxel size of 1.2*1.2*1.2 mm^3. Diffusion weighted imaging was performed twice and five b=0 volumes were acquired.

■ MRI data analysis

MRI examination and image analysis were completed in blinded fashion, but the group allocation of each lamb was not blinded during the final statistical analysis. Images acquired from T_1, T_2 and SWI scans were used to review brain injuries, such as infarcts and haemorrhage. DTI images were converted into NIFTI format, and then a brain mask was manually placed over the image using the FMRIB Software Library (FSL, FMRIB, Oxford, UK [11]). DTI data were corrected for eddy-current distortion, and then DTI parametric maps: fractional diffusivity (FA), axial diffusivity (AD), radial diffusivity (RD) and mean diffusivity (MD) were created with the Diffusion Toolbox of FMRIB. AD

was used as the largest eigenvalue of the tensor and RD was used as the average of the second and third eigenvalues of the tensor. Then all maps were co-registered with high-resolution T_2 images of each brain, using Linear Image Registration Tool (FLIRT [12]). The *b*0 image was used as the reference for co-registration.

In contrast to our previous studies [9,10], we only included MR images cropped to the right hemisphere to accurately compare MRI with the corresponding region used for histology. The regions we compared were the thalamus (Th), internal capsule (IC) and periventricular white matter (PVWM) derived from coronal slices, to increase the accuracy of matching and comparison with histological sections.

ROIs were defined manually on high-resolution T_2 images and then exported to the FA, AD, MD and RD maps to calculate the regional mean values for each lamb. ROIs were placed in the specific regions of the Th, IC and PVWM (SUPPLEMENTAL FIGURE I). The Sheep Brain Atlas from Michigan State University (Brain Biodiversity Bank, National Science Foundation) was utilised for accurate identification of anatomical regions. In each region, the mean value of the adjacent four to five slices that defined a given ROI volume was calculated for each of the ROIs to test between-animal variability in diffusivity for all groups.

Tissue Collection

At the end of the study, preterm lambs (125 ± 2 d) were humanely killed with an overdose of sodium pentobarbitone (>100 mg/kg i.v.) and their brains were excised. The cerebrum was halved along the midline and the right cerebral hemisphere was immersed in 4% paraformaldehyde (PFA) for 24 h and was then cut coronally into 5 mm-thick blocks and fixed in PFA for another six days prior to paraffin processing. Blocks were chosen and serially sectioned (8 μm thick) to match T_2 MRI images acquired from the Th, IC and PVWM to allow comparison.

■ Brain Immunohistochemistry

Coronal sections (n=1 section per immunohistochemical stain per brain) were stained with the following antibodies: NeuN (1:1000; Millipore, USA) to quantify neuronal density in the Th and myelin basic protein (MBP; 1:100; Millipore, USA) to assess myelin density in the IC and PVWM regions. Before incubation with anti-NeuN and anti-MBP, sections were treated with citrate buffer (pH 6.0) in a microwave oven and subsequently

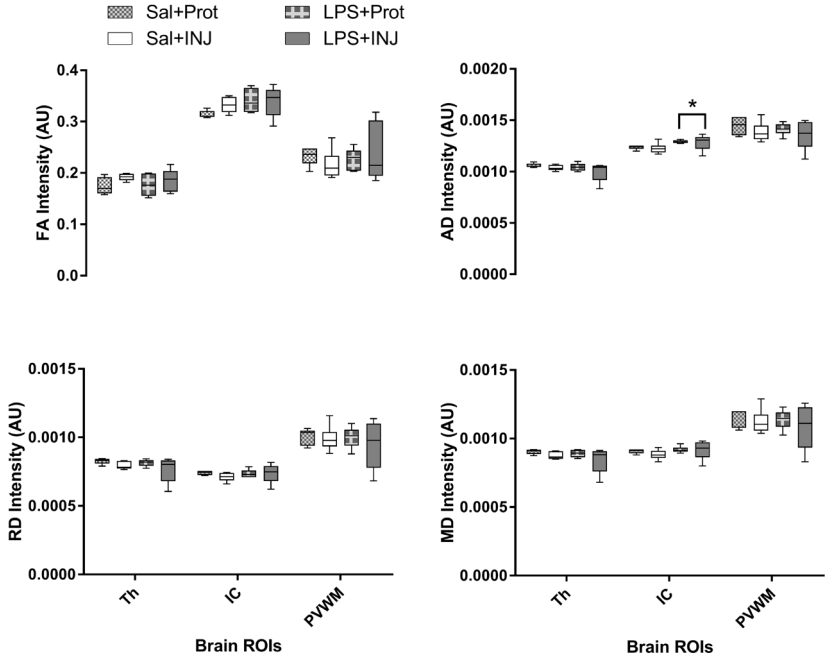

Figure 1. Mean DTI intensities in white matter regions. Mean FA, AD, RD and MD measurements for thalamus (Th), internal capsule (IC) and periventricular white matter (PVWM). Mean (box indicates 5-95% interval of the mean) with max-min error bars.
* $P<0.01$

incubated with hydrogen peroxide (0.3% in phosphate buffered saline) to block endogenous peroxidases. All sections were incubated with appropriate biotinylated secondary antibodies (1:200) and reacted using the Vectastain Elite ABC kit (1:1:200; 60 min; Vector Laboratories, Burlingame, CA, USA). No staining was present in sections when the primary antibody was omitted.

■ Quantitative analysis

Analyses were performed at equivalent sites within the cerebral white matter in each animal to maintain consistency. Histological ROIs were matched to T_2 MRI images to ensure accurate comparison. Slides were coded and the observer was blinded to the treatment group. Area density (cells/mm^2) of NeuN-positive neurons was counted in 3 random non-overlapping fields in the Th using ImageScope software (Aperio Technologies, California, USA). The intensity of MBP-immunoreactivity in the IC and PVWM was determined using previously validated optical density analysis [13]. For each section a correction was applied by subtracting the optical density measurement from a region of background staining. Optical density was assessed in two fields of view from equivalent regions of the IC and PVWM. For both NeuN- and MBP-immunoreactivity, the mean was calculated within each region for each animal and then a group mean determined. Only the right hemisphere was analysed for histological assessment.

Statistical Analyses

Mean tensor values were calculated from ROIs placed on the right side of Th, IC and PVWM on multiple adjacent coronal slices of DTI images (SUPPLEMENTAL FIGURE I) and then correlated with immunohistochemistry. The mean +/- SEM of the voxel intensities across all groups were then calculated, and two-way ANOVAs were used to compare the effects of LPS and ventilation strategy (post-hoc) with the significance level set at $P<0.05$. Data from the defined ROIs are presented as mean (box plot with 5-95% confidence interval of the mean) with maximum-minimum error bars. Scores obtained from immunohistochemistry were analysed by two-way ANOVA followed by Holm-Sidak post-hoc test as appropriate. Correlation analyses were performed using linear regression between DTI indices and immunohistochemistry scores using GraphPad Prism software (version 1.48, NIH, US).

Results

■ Physiological parameters

Blood gases and haemodynamic data were recorded throughout the experiment and have previously been reported [9,10]. In brief, 15 min after delivery Sal+INJ lambs had higher PIP (P=0.01) and lower PEEP (P=0.0001) compared to the Sal+PROT group. However, lambs groups did not differ in heart rate, SpO_2, blood gas and haemodynamic parameters [9,10] (SUPPLEMENTAL TABLE I). At 60 min from delivery, the start of imaging, the Sal+INJ lambs had higher PIP (P=0.02) but not in PEEP (P=0.6) compared to the Sal+PROT group. Further, there were no significant differences between lamb groups with regards to heart rate, SpO_2, blood gas and haemodynamic parameters at 60 min after delivery during the imaging [9,10] (SUPPLEMENTAL TABLE I).

■ Results of ROI analysis for DTI

In the right cerebral hemispheres, AD values in the IC were slightly, but significantly higher in LPS lambs compared to saline-treated lambs (F=8.275, P=0.01). However, no significant effect of injurious ventilation was found (FIGURE 1 and SUPPLEMENTAL TABLE II).

RD, FA and MD were not different between LPS and saline-treated lambs, with the exception of a trend for elevated FA in the IC of LPS lambs (F=3.377, P=0.08). These findings suggest that intrauterine inflammation specifically impaired axonal density and or organisation in the IC of the preterm lamb. Injurious ventilation tended to reduce RD and MD values in the Th (P=0.07 and P=0.08, respectively), while the effect of LPS was not significant (P=0.35 and P=0.3, respectively). There were no significant differences in FA, AD, RD and MD in the PVWM region to indicate a treatment effect, but the PVWM was highly variable for all DTI indices in the LPS+INJ group (FIGURE 1).

■ Immunohistochemistry scores

MBP-positive immunoreactivity in the IC was significantly decreased after LPS (FIGURE 2; F=5.765, P=0.02), but was not influenced by injurious ventilation (FIGURE 3A, F=0.00638, P=0.9). This effect of LPS was not mirrored in

the PVWM (FIGURE 3B, F=0.7933, P=0.38). The density of NeuN-positive neurons was not significantly different in the Th (FIGURE 4) when testing the effects of either LPS or injurious ventilation (FIGURE 3C, P=0.8 and P=0.4, respectively).

■ Correlation between DTI and immunohistochemistry

The correlations between DTI diffusivity and histology scores were highly variable in relation to the effects of injurious ventilation and LPS within specific white matter regions. However, we found a significant inverse correlation between FA values and MBP staining in PVWM across groups (FIGURE 5, r=-0.268, P=0.01), and a trend towards a correlation in the IC (SUPPLEMENTAL FIGURE IIB, r=-0.1527, P=0.07). There was no significant correlation between FA values and histopathological density of NeuN-positive neurons in the Th (SUPPLEMENTAL FIGURE IIA, r=0.0488, P=0.3). Interestingly, AD, RD and MD indices were independent of NeuN and MBP scores in the Th, IC and PVWM. These DTI indices were similar regardless of the presence of myelin defects in the white matter of preterm neonates exposed to LPS, and did not appear to be exacerbated by injurious ventilation in any of the ROIs examined (SUPPLEMENTAL FIGURE II).

Discussion

Preterm neonates exposed to intrauterine inflammation are at increased risk of ventilation-induced brain inflammation and injury [7,8]. We have previously determined that a threshold-based DTI mapping approach revealed the exacerbation of injury induced by the combined effects of intrauterine inflammation and inappropriate ventilation strategies at birth (FIGURE 6). In this study, we examined whether the injury detected using this technique correlated with histological analyses. We found that several DTI indices correlated with the histopathological changes in myelin density caused by perinatal inflammation in vulnerable white matter regions. However, no effect of ventilation strategy was observed. There was no evidence of exacerbation of brain injury due to the combined effects of inflammation and injurious ventilation at this acute time point.

Until now there have been few studies that have investigated whether MRI approaches are sensitive enough to detect the acute phase of brain injury *in vivo* using widely available 3T clinical MRI scanners [14-16], and even fewer studies that have validated such imaging approaches with histopathological assessment [17,18]. DTI is an accepted MRI method based on measures of water diffusion within brain tissues and has been shown to provide

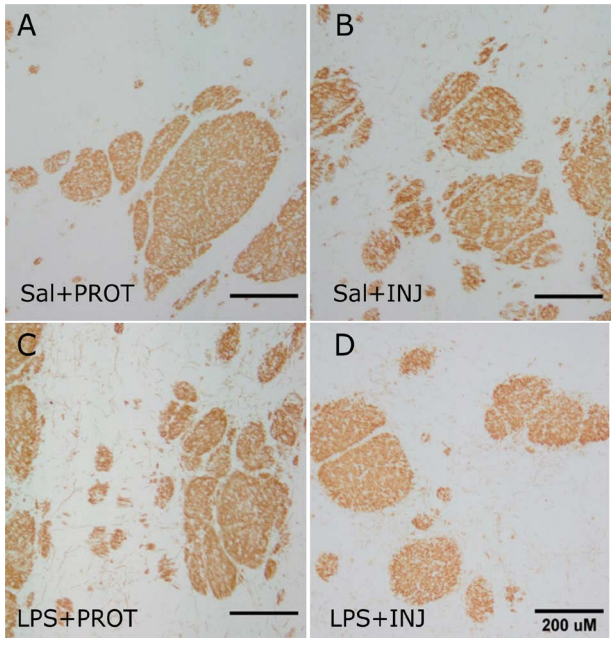

Figure 2 A-D. Representative myelin basic protein staining in the internal capsule (IC) regions in the Sal+PROT, Sal+INJ, LPS+PROT and LPS+INJ groups.
Scale bar indicates 200 μm

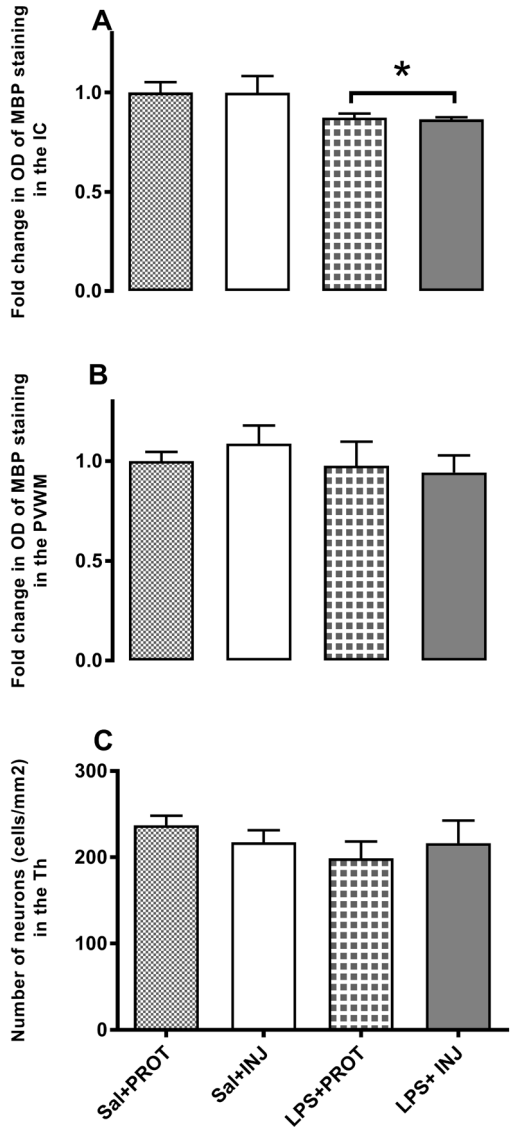

Figure 3. Assessment of neuronal density and myelin density by immunohistochemistry in white matter regions. A and **B:** Assessment of the fold change in the optical density (OD) of myelin basic protein (MBP) staining in two fields of view from equivalent regions of the internal capsule (IC) and periventricular white matter (PVWM), respectively. **C:** Quantification of neuronal density in the thalamus (Th).
***P**<0.02

quantitative information about microstructural changes that correlated with myelination in the neonatal brain [19].

We found that DTI indices were somewhat variable in the three white matter regions examined in this study. Notably, in all lambs fractional anisotropy was much higher in the IC than the Th or PVWM in this study (FIGURE 1). Recently, Rose et al. [20] suggested that in preterm human neonates higher FA in the IC compared to other white matter regions might reflect earlier microstructural development in the IC as this region shows initiation of myelination preterm at ≤ 32 weeks gestational age. We now show that even after taking into account the higher FA in the IC of all preterm lambs, the FA and axial diffusivity indices were elevated in the white matter of the IC due to localised inflammation that evolved over one week prior to delivery. However, diffusivity measures based on these small ROIs were less sensitive to the effect of acute exposure to injurious ventilation. Intra-amniotic LPS-induced inflammation reduced myelin density in the IC and PVWM regions (FIGURES 2 and 3), as previously reported [21,22]. We

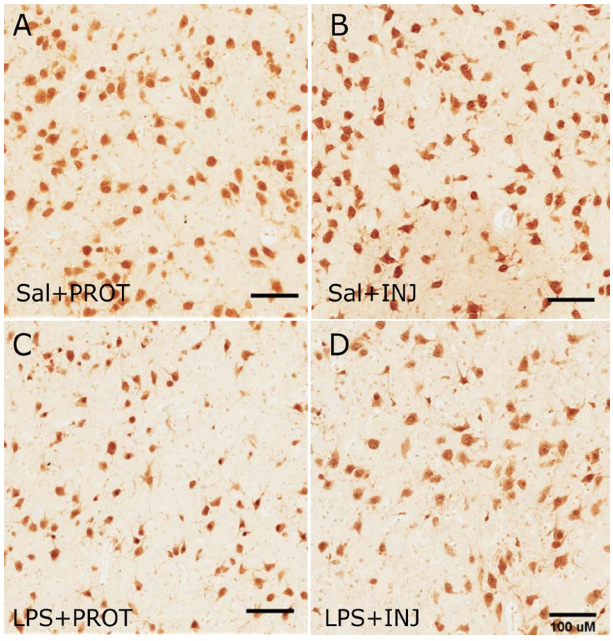

Figure 4 A-D. Representative NeuN staining in the thalamus (Th) in in the Sal+PROT, Sal+INJ, LPS+PROT and LPS+INJ groups.
Scale bar indicates 100 μm

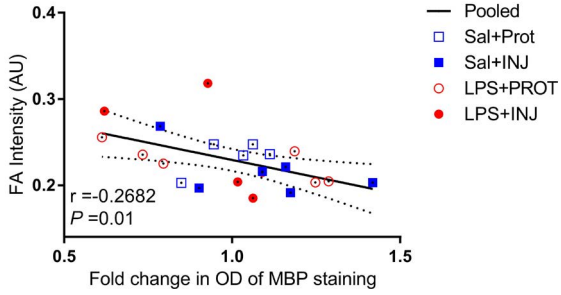

Figure 5. Correlation between fractional anisotropy (FA) and immunohistochemistry scores in preterm lambs.
Sal+PROT, open blue squares; Sal+INJ, closed blue squares; LPS+PROT, open red circles; LPS+INJ, closed red circles. The column display quantification of the fold change in the optical density (OD) of myelin basic protein (MBP) staining in two fields of view from equivalent regions of periventricular white matter. Solid and dotted lines represent the regression and 95% confidence intervals of the fit, respectively.

also suggest that increased axial diffusivity in these white matter regions probably occurs as a result of the decrease in axonal density, which increases the space surrounding axons and might therefore have led to the axons becoming straighter (less angular) [23]. This is consistent with our histological findings that demonstrate MBP-positive immunoreactivity in the IC was significantly decreased after LPS, suggesting neural degeneration or reduced neuron-parenchyma growth in this period.

There are two possible explanations for why the same DTI indices might have been less sensitive to ventilation induced injury in this study. First, the methodology of traditional ROI based DTI analysis approaches might not be sensitive enough to consistently detect the effect of injurious ventilation in the presence of ongoing inflammation at this early time point after delivery. In other words, there is the potential for small and dispersed injury sites to be overlooked when small ROIs or low resolution sequences are employed in simple comparisons of mean eigenvalues. Riddle et al. [24] have reported that detecting small brain injuries, such as microcysts, is hampered by the limited imaging resolutions achievable when undertaking *in vivo* studies using clinical MRI systems. Using the preterm lamb model, we have found that the threshold-based DTI mapping approach is more sensitive for the identification of voxels with low levels of diffusivity following

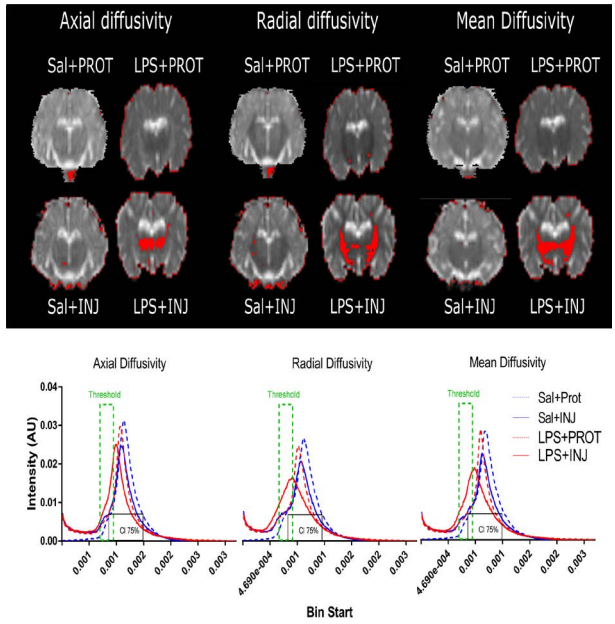

Figure 6. Examples whole brain DTI-colour maps of the thalamus in preterm lambs. A threshold-based DTI colour map technique describes the tensor orientation in relation to the white matter tract direction [10]. Histograms of axial diffusivity (AD), radial diffusivity (RD) and mean diffusivity (MD) for the whole individual brain in the two lambs exposed to LPS and two lambs without LPS treatment are plotted in the histograms (down). We manually highlighted lower diffusivity voxels (green dashed line) set below the 75th percentile of intensities in the protective lamb (Saline PROT), allowing the voxel diffusivity intensities falling below the low threshold display as red for AD, RD and MD measurements for the lamb exposed to intrauterine inflammation (LPS) and controls lambs not exposed to LPS. In the LPS+INJ, the extent of the low diffusion voxels (red overlay) was more visible on diffusion image for a slice passing through the thalamus, while the low AD and MD values were almost absent in same region in the Saline PROT, Saline INJ and LPS+PROT groups. Further, there was some small degree of low RD values in the thalamus of the Saline INJ and LPS+PROT lambs, but not in the Saline PROT lamb.

injurious ventilation [10], even though the mean diffusivities were not significantly altered in the white matter regions in that study. Bearing in mind that water diffusion through neurons in a given voxel is an index of neuronal activity [25], this raises the possibility that a reduction in mean diffusivities values of a given ROI due to ventilation injury only becomes evident in ROI based analyses when the distribution and number of voxels of low diffusivity increases with time. Second, it is reasonable to suggest that perhaps one hour after delivery is not sufficiently long for microstructural changes to develop from ventilation induced injury. The fact that there was no exacerbation of microstructure changes in the white matter due to the combined effects of injurious ventilation and inflammation in the LPS+INJ group in this acute phase suggests that in this study pathological changes were not consistently evoked by injurious ventilation or there was insufficient time for the inflammation to manifest as gross injury. The latter seems likely, since ROI based DTI analyses reveal significant depression in diffusivity of specific white matter regions in our preterm lamb model 24 hours post injurious ventilation (Alahmari, Polglase, Pearson, unpublished data, 2017). Further, a previous study investigating preterm infants detected brain injury with DTI based ROI after the first 4-6 days of postnatal life [26]. Therefore, both explanations might partly take into account the findings of this study.

In addition to the timing of imaging, the detection of ventilation-induced brain injury is highly likely to be determined by the field strength of the MRI system and the analysis approaches used and are therefore important considerations for future studies. Sensitivity is increased in very high field (7T) strength MRI systems as the strength of the scanner magnetic field determines transverse relaxation. Others have shown that very high field strength MRI can detect microscopic white matter injury *ex vivo* [24,27]. Hence, it is highly possible that currently available 7T clinical scanners have enhanced sensitivity for characterising white matter injury caused by risk factors associated

with preterm birth.

Conclusion

In conclusion, *in vivo* DTI was able to detect diffusivity changes associated with microstructural white matter impairment due to perinatal inflammation soon after delivery in preterm lambs. Further, there was an inverse correlation between FA and myelin density in the PVWM and to a lesser extent the IC regions. As the preterm lamb model is ideal for preclinical examination of the pathophysiology of brain lesions and the impact on subsequent postnatal neural function with MRI and electrophysiological techniques, further research is warranted to establish subacute timelines for high sensitivity detection of white matter injury after birth. Moreover, DTI techniques offer the potential for investigating the consequences of neural injury and the efficacy of early interventions in neonates *in vivo*.

Sources of Funding

This research was supported by a joint National Heart Foundation of Australia and National Health and Medical Research Council (NH&MRC) Career Development Fellowship (GRP: 1105526), an NHMRC-Australian Research Council Dementia Research Development Fellowship (SKB; 1110040), NHMRC CJ Martin Early Career Fellowship (1090890; RG), a Rebecca L. Cooper Medical Research Foundation Fellowship (GRP) and the Victorian Government's Operational Infrastructure Support Program. This research was supported by National Institute of Health R01HD072848-01A1

Disclosures

The funders had no role in study design, data collection and analysis, decision to publish, or preparation of the manuscript. The authors declare that they do not have any conflicts of interests.

REFERENCES

1. Polglase GR, Hooper SB. Role of intra-luminal pressure in regulating pbf in the fetus and after birth. *Curr. Pediatr. Rev.* 2, 287-99 (2006).
2. Polglase GR, Hillman N, Pillow JJ *et al.* Positive end-expiratory pressure and tidal volume during initial ventilation of preterm lambs. *Pediatr. Res.* 64, 517-522 (2008).
3. Polglase GR, Miller SL, Barton SK *et al.* Initiation of resuscitation with high tidal volumes causes cerebral hemodynamic disturbance, brain inflammation and injury in preterm lambs. *PLoS. One.* 7 (2012).
4. Lahra MM, Jeffery HE. A fetal response to chorioamnionitis is associated with early survival after preterm birth. *Am. J. Obstet. Gynecol.* 190, 147-151 (2004).
5. Shatrov J, Birch S, Lam L *et al.* Chorioamnionitis and cerebral palsy: a meta-analysis. *Obstet. Gynecol*. 116, 387-392 (2010).
6. Stark MJ, Hodyl NA, Belegar V KK *et al.* Intrauterine inflammation, cerebral oxygen consumption and susceptibility to early brain injury in very preterm newborns. *Arch. Dis. Child. Fetal. Neonatal. Ed.* 101, F137-F42 (2016).
7. Polglase GR, Nitsos I, Baburamani AA *et al.* Inflammation in utero exacerbates ventilation-induced brain injury in preterm lambs. *J. Appl. Physiol. (1985).* 112, 481-489 (2012).
8. Barton SK, Moss TJM, Hooper SB *et al.* Protective ventilation of preterm lambs exposed to acute chorioamnionitis does not reduce ventilation-induced lung or brain injury. *PLoS. ONE.* 9, e112402 (2014).
9. Skiold B, Wu Q, Hooper SB *et al.* Early detection of ventilation-induced brain injury using magnetic resonance spectroscopy and diffusion tensor imaging: an in vivo study in preterm lambs. *PLoS. One*. 9, e95804 (2014).
10. Alahmari DM, Skiöld B, Barton SK *et al.* Diffusion tensor imaging colour mapping threshold for identification of ventilation-induced brain injury after intrauterine inflammation in preterm lambs. *Front. Pediatr.* 5 (2017).
11. Jenkinson M, Beckmann CF, Behrens TEJ *et al.* FSL. *Neuroimage*. 62, 782-790 (2012).
12. Jenkinson M, Bannister P, Brady M *et al.* Improved optimization for the robust and accurate linear registration and motion correction of brain images. *Neuroimage.* 17, 825-841 (2002).
13. Atik A, Cheong J, Harding R *et al.* Impact of daily high-dose caffeine exposure on developing white matter of the immature ovine brain. *Pediatr. Res.*76, 54-63 (2014).
14. Rose J, Vassar R, Cahill-Rowley K *et al.* Neonatal physiological correlates of near-term brain development on mri and dti in very-low-birth-weight preterm infants. *NeuroImage*. 5, 169-177 (2014).
15. Shim SY, Jeong HJ, Son DW *et al.* Altered microstructure of white matter except the corpus callosum is independent of prematurity. *Neonatology*. 102, 309-315 (2012).
16. Anblagan D, Pataky R, Evans MJ *et al.* Association between preterm brain injury and exposure to chorioamnionitis during fetal life. *Sci. Rep*. 6, 37932 (2016).
17. Choe AS, Stepniewska I, Colvin DC *et al.* Validation of diffusion tensor MRI in the central nervous system using light microscopy: Quantitative comparison of fiber properties. *NMR. Biomed.* 25, 900-908 (2012).
18. Wei PT, Leong D, Calabrese E *et al.* Diffusion tensor imaging of neural tissue organization: Correlations between radiologic and histologic parameters. *Neuroradiol. J.* 26, 501-510 (2013).
19. Liu Y, Aeby A, Baleriaux D *et al.* White matter abnormalities are related to microstructural changes in preterm neonates at term-equivalent age: a diffusion tensor imaging and probabilistic tractography study. *AJNR. Am. J. Neuroradiol.* 33, 839-845 (2012).
20. Rose J, Vassar R, Cahill-Rowley K *et al.* Brain microstructural development at near-term age in very-low-birth-weight preterm infants: an atlas-based diffusion imaging study. *Neuroimage.* 86, 244-256 (2014).
21. Dean JM, van de Looij Y, Sizonenko SV *et al.* Delayed cortical impairment following lipopolysaccharide exposure in preterm fetal sheep. *Ann. Neurol.* 70, 846-856 (2011).
22. Gavilanes AWD, Strackx E, Kramer BW *et al.* Chorioamnionitis induced by intra-amniotic lipopolysaccharide resulted in an interval-dependent increase in central nervous system injury in the fetal sheep. *Am. J. Obstet. Gynecol.* 200, 437.e1-437.e8 (2009).
23. Takahashi M, Ono J, Harada K *et al.* Diffusional anisotropy in cranial nerves with maturation: quantitative evaluation with diffusion MR imaging in rats. *Radiology.* 216, 881-885 (2000).
24. Riddle A, Dean J, Buser JR *et al.* Histopathological correlates of magnetic resonance imaging-defined chronic perinatal white matter injury. *Ann. Neurol.* 70, 493-507 (2011).
25. Le Bihan D, Urayama S-i, Aso T *et al.* Direct

and fast detection of neuronal activation in the human brain with diffusion MRI. *Proc. Natl. Acad. Sci. USA.* 103, 8263-8268 (2006).

26. Ancora G, Testa C, Grandi S *et al.* Prognostic value of brain proton mr spectroscopy and diffusion tensor imaging in newborns with hypoxic-ischemic encephalopathy treated by brain cooling. *Neuroradiology.* 55, 1017-1025 (2013).

27. Pitt D, Boster A, Pei W *et al.* Imaging cortical lesions in multiple sclerosis with ultra-high-field magnetic resonance imaging. *Arch. Neurol.* 67, 812-818 (2010).